

Article

Effect of Acid-Injection Mode on Conductivity for Acid-Fracturing Stimulation in Ultra-Deep Tight Carbonate Reservoirs

Jiangyu Liu ^{1,2,3}, Dengfeng Ren ^{1,2,3}, Shaobo Feng ^{1,2,3}, Ju Liu ^{1,2,3}, Shiyong Qin ^{1,2,3}, Xin Qiao ^{1,2,3} and Bo Gou ^{4,*} 

- ¹ Oil and Gas Engineering Research Institute, Tarim Oilfield Company, PetroChina, Korla 841000, China; ljyu-tlm@petrochina.com.cn (J.L.); rdf-tlm@petrochina.com.cn (D.R.); fengsb-tlm@petrochina.com.cn (S.F.); liuju-tlm@petrochina.com.cn (J.L.); qinsy-tlm@petrochina.com.cn (S.Q.); qiaoxin-tlm@petrochina.com.cn (X.Q.)
- ² R&D Center for Ultra Deep Complex Reservoir Exploration and Development, CNPC, Korla 841000, China
- ³ Engineering Research Center for Ultra-Deep Complex Oil and Gas Reservoir Exploration and Development, Xinjiang Uygur Autonomous Region, Korla 841000, China
- ⁴ National Key Laboratory of Oil and Gas Reservoir Geology and Exploitation, Southwest Petroleum University, Chengdu 610500, China
- * Correspondence: bogou@swpu.edu.cn

Abstract: The conductivity of acid-etched fractures and the subsequent production response are influenced by the injection mode of the fracturing fluid and acid fluid during acid fracturing in a carbonate reservoir. However, there has been a lack of comprehensive and systematic experimental research on the impact of commonly used injection modes in oilfields on conductivity, which directly affects the optimal selection of acid-fracturing injection modes. To address this gap, the present study focuses on underground rock samples, acid systems, and fracturing fluid obtained from ultra-deep carbonate reservoirs in the Fuman Oilfield. Experimental investigations were conducted to examine the conductivity of hydraulic fractures etched by various types of acid fluids under five different injection modes: fracturing fluid + self-generating acid or cross-linked acid; fracturing fluid + self-generating acid + cross-linked acid. The findings demonstrate that the implementation of multi-stage alternating acid injection results in the formation of communication channels, vugular pore space, and natural micro-cracks, as well as grooves and fish-scales due to enhanced etching effects. The elevation change, amount of dissolved rock, and conductivity exhibited by rock plates are significantly higher in comparison to those achieved through the single-acid injection mode while maintaining superior conductivity. It is recommended for optimal conductivity and retention rate in the Fuman Oilfield to adopt two stages of alternating acid-fracturing injection mode. Field application demonstrated that two-stages of alternating acid-fracturing generate more pronounced production response than the adjacent wells.

Keywords: ultra-deep carbonate reservoirs; acid-injection mode; multi-stages alternating acid fracturing; acid-fracture morphology; conductivity; field application



Citation: Liu, J.; Ren, D.; Feng, S.; Liu, J.; Qin, S.; Qiao, X.; Gou, B. Effect of Acid-Injection Mode on Conductivity for Acid-Fracturing Stimulation in Ultra-Deep Tight Carbonate Reservoirs. *Processes* **2024**, *12*, 651. <https://doi.org/10.3390/pr12040651>

Academic Editor: Qibin Li

Received: 27 February 2024

Revised: 19 March 2024

Accepted: 21 March 2024

Published: 25 March 2024



Copyright: © 2024 by the authors. Licensee MDPI, Basel, Switzerland. This article is an open access article distributed under the terms and conditions of the Creative Commons Attribution (CC BY) license (<https://creativecommons.org/licenses/by/4.0/>).

1. Introduction

The deep and ultra-deep carbonate reservoirs currently represent the focal areas of oil and gas exploration in China. These reservoirs are characterized by extensive lithologic or structure-lithologic complex gas or oil fields, such as those found in the Puguang, Yuanba Changxing-Feixianguan, and Anyue-Penglai Dengying formations in the Sichuan Basin, as well as the Shunbei and Fuman Ordovician formations in the Tarim Basin. Additionally, significant exploration is taking place around the Tongyuan fault within the Moxi Longwangmiao formation in the Sichuan Basin. Moreover, deep and ultra-deep carbonate reservoirs have emerged as the cornerstone for the expansion of oil and gas production in these basins [1]. The deep carbonate reservoir exhibits strong heterogeneity, with

uneven distribution of natural oil- and gas-rich fracture-vug in space, which often poses challenges in achieving industrial production following drilling. Acid fracturing emerges as a pivotal technology for enhancing production in deep carbonate reservoirs. By creating acid-fractures, this technique effectively connects the discontinuous oil and gas reservoirs, enabling the commercial production of oil and gas wells [2].

The acid penetration range and fracture conductivity are crucial factors impacting the productivity of a fractured well. However, conductivity holds greater significance as only acid-etched fracture with a specific level of conductivity makes a significant contribution to productivity [3]. The factors influencing conductivity primarily encompass geological aspects, such as reservoir temperature, rock and mineral composition and distribution, as well as natural fracture development [4]. These inherent reservoir characteristics are difficult to adjust. On the other hand, engineering factors involve the acid system, acid-injection parameters (including injection rate and time), and acid-injection processes (such as injection mode selection). Enhancing the parameters of acid-fracturing engineering factors represents a crucial approach for regulating the acid-fracture conductivity.

The enhancement of acid-fracture conductivity has been extensively investigated by many scholars, and can generally be categorized into three main areas. First, hybrid fracturing with the combination of acid fracturing and proppant fracturing can enhance the acid-fracture conductivity [5,6]. However, proppant fracturing may pose challenges in terms of proppant injection and even introduce potential engineering risks associated with proppant plugging in ultra-deep tight carbonate reservoirs. Second, the utilization of additional agents enhances the mechanical strength of rock support points on the acid-fracture surface, thereby improving conductivity [7,8]. This method is relatively novel and is currently undergoing exploration and trial. Last, adjusting both acid-injection parameters and their corresponding mode helps to increase roughness on acid-fracture topography, thereby enhancing fracture conductivity [9–11]. This simple yet effective method can be easily implemented in the field.

Conventional gelled acid fracturing exhibits limited penetration distance and conductivity in deep carbonate reservoirs subjected to high formation temperatures (>150 °C) and closure pressure (>50 MPa), posing challenges in meeting long-term production requirements [12]. In order to enhance the acid penetration distance and conductivity, the pre-pad acid-fracturing mode is commonly employed. This pre-fluid typically consists of a fracturing fluid or weakly reactive autogenic acid, primarily utilized for creating and cooling a fracture. The frequently used acid systems include gelling acid and crosslinked acid, which are mainly applied for etching hydraulic fractures and generating conductivity. This injection mode is straightforward to implement on-site and extensively utilized in the initial stages of acid-fracturing development [13,14]. Multistage alternating acid fracturing is an enhanced mode of pre-pad acid fracturing, employing alternate stages of pad fluid and acid. It currently stands as the primary deep-penetrating acid-fracturing technology [9,15,16]. Compared to conventional gelled acid fracturing and pre-pad acid fracturing, multi-stage alternating acid fracturing has the following obvious advantages: first, the introduction of high viscosity fracturing fluid into the fracture reduces the acid leakoff in wormholes and natural fractures [9,15]; second, the non-reactive fracturing fluid or weakly reactive autogenic acid can effectively lower the acid-rock reaction temperature and increase the acid penetration distance [17,18]; third, the viscosity difference between the fracturing fluid and acid facilitates the occurrence of a viscous fingering phenomenon, creating non-uniform etching on the fracture surfaces and thereby improving the conductivity of acid-etched fractures [10].

The stimulation fluids and injection modes employed in different acid fracturing exhibit significant variations, and many scholars have demonstrated that these disparities directly impact the acid-fracture morphology as well as the conductivity. Lungwitz, B. et al. found that differential etching resulted in higher conductivity with self-diverting-acid than that observed with straight HCl [19]. Navarrete et al. found emulsified acid produced higher conductivities than straight acid at high closure stresses, in spite of larger etched

widths, providing a more efficient use of the acid [20]. Tariq et al. observed that rock hardness and roughness had a significant impact on fracture conductivity. Also, the type of treating fluid and rock determined the generated rock roughness, where higher reactivity resulted in higher roughness and hence conductivity [21]. Sui et al. found that as the experimental ambient temperature increased, the conductivity of the acid-etching fracture gradually increased [22].

The experimental investigation of the aforementioned single acid system demonstrates that the acid type and temperature exert an influence on both the etching morphology and conductivity. The multistage alternating acid-fracturing mode also has an impact on the acid-etching morphology and conductivity. Ren et al. found that the acid types can strongly affect both the fracture conductivity and etching patterns during alternating injection [23]. The acid-fracture conductivity generated by alternative stages with autogenic acid and gelled acid was influenced by the initial fracture morphology and temperature, as observed in the study conducted by Gou et al. [17], while the alternate injection of gelled acid and cross-linked acid combination, as discovered by Zhu et al., can create complex etching channels, resulting in the generation of high fracture conductivity in the porous carbonate reservoir [24].

The above experiments reveal that both the selection of the acid system and mode of acid injection significantly affect not only the acid-etched fracture morphology but also its conductivity. Nevertheless, current research predominantly concentrates on investigating a single mode of acid injection while seldom comparing variations in acid-fracture conductivity across different modes within rock samples from identical blocks. This lack of comprehensive and systematic analysis hinders our understanding of how different acid-injection modes influence conductivity and impede effective selection of appropriate acid-injection modes in oilfields. To address this knowledge gap, acid etching and conductivity tests were conducted on the underground cores of ultra-deep carbonate reservoirs in the Fuman Oilfield. These tests revealed valuable insights into the characteristics of acid-etching fracture morphology and conductivity under various conditions of acid-injection modes, thereby providing crucial support for the selection of acid-fracturing treatment in the field.

2. Experimental Methodology

2.1. Experimental Materials

The Fuman Oilfield in the Tarim Basin is situated at the subsidence center of both the Nanhua fault basin and the Sinian depression basin, with its target layer being Yijianfang Formation limestone buried at a depth ranging from 6500 to 8200 m. The formation temperature ranges between 146.9 °C and 163.9 °C, while the porosity of the downhole core varies from 0.54% to 7.46%, and the permeability ranges from 0.0079 to 91 mD [25].

The experimental rock samples were selected from downhole cores of the Yifangfang Formation in the Fuman Oilfield (Figure 1a). According to API standards, these samples were cut into rectangle shapes measuring 175.0 ± 0.2 mm in length, 35.0 ± 0.2 mm in width, and 50.0 ± 0.2 mm in thickness. In order to simulate underground rough hydraulic fractures, researchers often employ the Brazilian splitting method for rock sample preparation [17]. However, due to the small size and the susceptibility to damage of downhole cores, these cores have to be processed into rectangular polished rock slabs as in Figure 1b. This processing not only eliminates interference from initial hydraulic fracture morphology in experiments but also maximizes the impact of different acid-injection modes on etching morphology and flow conductivity.

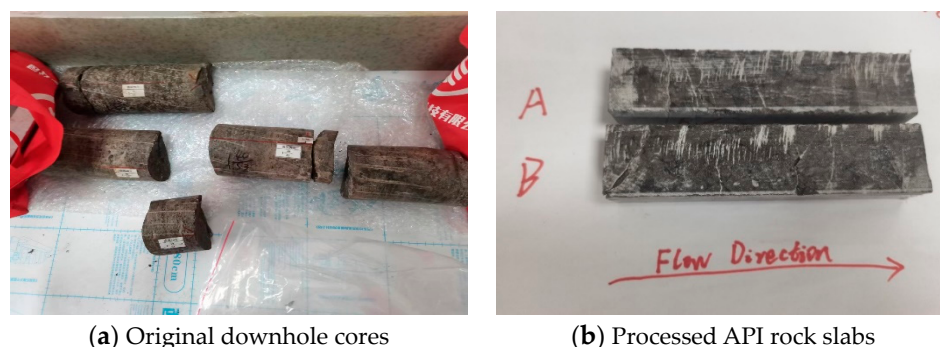


Figure 1. Downhole cores and processed rock slabs. Note: A is upper slab, and B is lower slab.

The self-generating acid, cross-linked acid, gelled acid, and fracturing fluid utilized in the experiment were sourced from the Fuman Oilfield field, with their respective basic formulas presented in Table 1.

Table 1. Formulation of fracturing fluid and acid system using in Fuman Oilfield.

Acid System	Formulation
Fracturing fluid	0.45% super gum + 1% demulsifier + 1% cleanup additive + 0.5% temperature stabilizer + 0.08% pH regulator + 0.1% bactericide + 0.8% cross-linking agent + 0.02% ammonium persulfate
Self-generating acid	A agent:B agent = 1:1
Cross-linked acid	20.0% HCl + 0.8% thickener + 0.5% demulsifier + 0.5% diverting agent + 2.0% corrosion inhibitors + 1.0% iron ion stabilizer + 0.5% conditioner + 0.8% cross-linking agent
Gelled acid	20.0% HCl + 0.8% thickener + 0.5% demulsifier + 0.5% diverting agent + 2.0% corrosion inhibitors + 1.0% iron ion stabilizer + 0.5% conditioner

2.2. Experimental Sets

Acid-fracture conductivity test equipment consists of three modules, namely, the acid-etching hydraulic fracture module, the fracture laser scanning 3D imaging module and the conductivity test module in Figure 2 [17]. The three equipment modules serve different simulation functions, with the acid-etching simulation module designed to replicate the process of acid etching during acid fracturing. The laser scanning 3D imaging module is used to capture the hydraulic fracture morphology before and after acid etching. Lastly, the conductivity test module assesses the acid-fracture conductivity under closure pressure.



Figure 2. Acid-fracture conductivity test equipment.

2.3. Experimental Schedule Design

In order to match the reservoir conditions with the experimental test conditions of acid-fracture conductivity, the three key parameters primarily considered are the acid-injection displacement, the acid-injection time, and the acid-rock reaction temperature.

2.3.1. Injection Displacement and Time

The injection displacement (mL/min) at the laboratory experimental scale cannot be consistent with the injection displacement (m³/min) at the field scale due to limitations in device injection capacity and rock sample size. The acid-injection displacement at the engineering scale is often downscaled to the laboratory experimental scale based on the Reynolds number similarity criterion. The conversion formula is as follows [17]:

$$q_1 = \frac{q_f h_1}{2h_f} \left(\frac{w_f}{w_1} \right)^{\frac{2n-2}{2-n}} \quad (1)$$

where q_1 is the experimental acid-injection displacement, mL/min; q_f is the acid-injection displacement in the field, m³/min; w_1 is the experimental fracture width, m; w_f is the field fracture width, m; h_1 is the experimental fracture height, m; h_f is the field fracture height, m; n is the flow characteristics of the index.

The field acid-injection displacement is scaled down to the experimental acid-injection displacement based on the rheological parameter characteristics and acid-injection rate of self-generating acid and cross-linked acid in the Fuman Oilfield within the research area, as per Formula (1). The corresponding results are presented in Table 2.

Table 2. Conversion of field engineering scale into laboratory experimental scale displacement.

Self-Generating Acid ($n = 0.125$)		Cross-Linked Acid ($n = 0.295$)	
Field, m ³ /min	Laboratory, mL/min	Field, m ³ /min	Laboratory, mL/min
4.5	157	4.5	195
5.5	189	5.5	216
6.0	209	6.0	260

As shown in Table 2, the self-generating acid-injection displacement of Fuman Oilfield ranges from 4.5 to 6.0 m³/min, which is equivalent to an experimental acid-injection rate of 157–260 mL/min. The experimental design of self-generating acid and cross-linked acid uses an average experimental acid-injection rate of 200 mL/min. The acid-injection rate of terminal gelled acid (uncross-linked cross-linked acid) is set at 100 mL/min to simulate the process of close acidizing fracture.

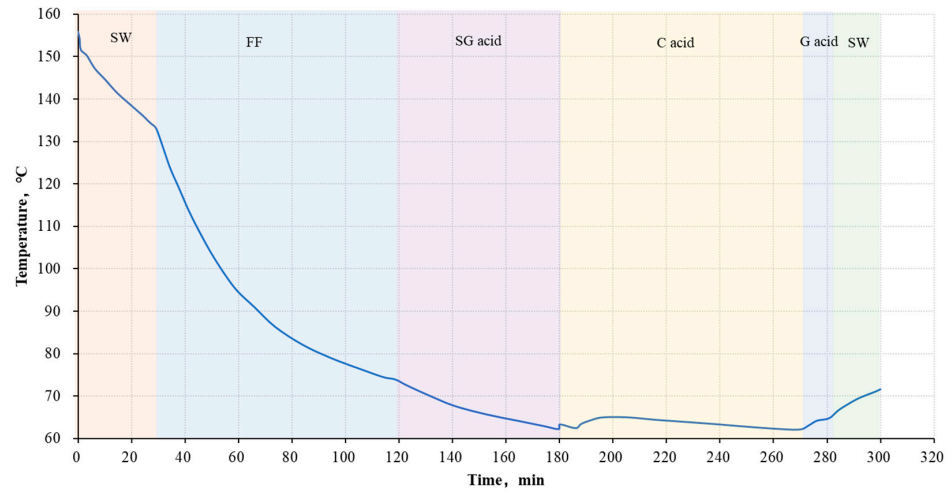
Acid-injection time is determined based on the standard acid-injection scale and acid-injection rate in the Fuman Oilfield. The duration for self-generating acid is 60 min, cross-linked acid requires 90 min, and gelled acid needs only 10 min.

2.3.2. Acid-Rock Reaction Temperature

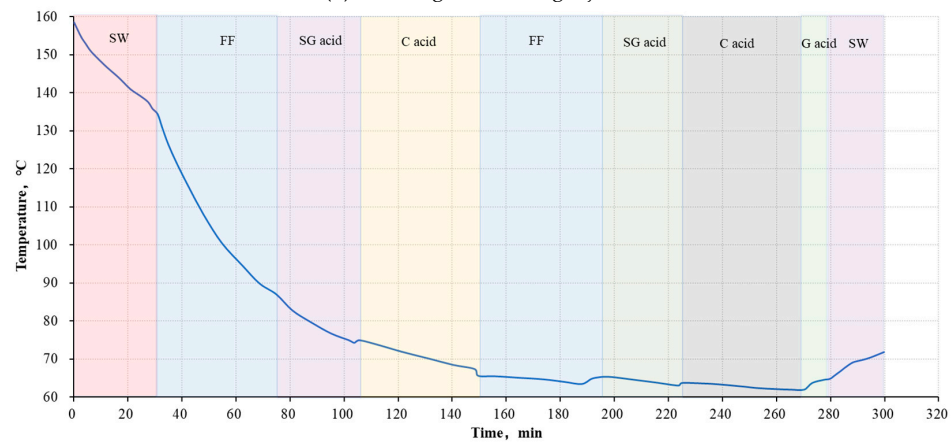
Temperature exerts a significant effect on the acid-rock reaction of carbonate rocks, particularly in ultra-deep and high-temperature reservoirs.

Based on the typical injection volume (1000–2000 m³) in single well acid fracturing at the Fuman Oilfield, the numerical simulation calculation method was employed to simulate the underground temperature field variations during different alternating stages with a certain total injection volume [26], which was used to determine the temperature of the acid-rock reaction. The distribution of each type of fluid in each alternating stage was evenly balanced based on the alternating series when there were changes in the alternate stages. The underground temperature change resulting from the alternating injection of slick water + fracturing fluid + self-generating acid + cross-linked acid + gelled acid (closed acidizing) at a total injection volume of 1750 m³ is illustrated in Figure 3. In this process,

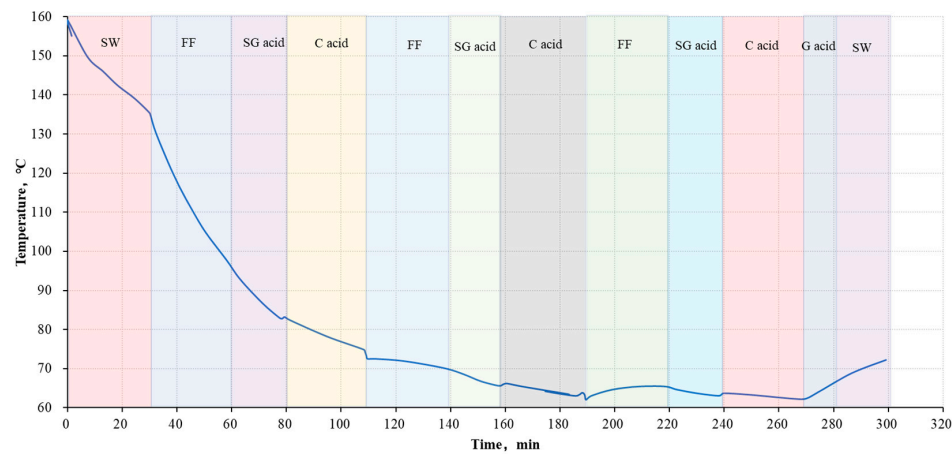
slick water 450 m³ and fracturing fluid 450 m³ are used to cool the formation and create fractures. Self-generating acid with a volume of 300 m³ is employed to etch the far end of the hydraulic fracture, while cross-linked acid at 450 m³ is used to etch the middle section. Additionally, gelled acid 25 m³ is applied for closed acidizing to enhance the conductivity near the wellbore. Finally, a displacement fluid of 75 m³ displaces both surface and wellbore acids into the formation.



(a) One-stage alternating injection



(b) Two-stage alternating injection



(c) Three-stage alternating injection

Figure 3. Variation of bottom temperature under different alternate stages. Note: SW is slick water, FF is fracturing fluid, SG acid is self-generating acid, C acid is cross-linked acid, and G acid is gelled acid.

The variation of underground temperature caused by different alternating injection modes is quite different, as depicted in Figure 3, under the condition of the same injection volume. In Figure 3a, it can be observed that when employing non-reactive pre-pad fracturing (i.e., one-stage alternating injection), the formation temperature during the slick water and fracturing fluid injection reaches 75 °C, which corresponds to the initial temperature for self-generating acid-rock reaction. Subsequently, upon complete injection of self-generating acid, the formation temperature drops to 60 °C, representing the initial temperature for the cross-linked acid-rock reaction. Similarly, from Figure 3b,c, we obtained fracture temperatures for two-stage and three-stage alternating acid-etching experiments, respectively, which are listed in Table 3.

Table 3. Acid-etching experimental scheme.

Rock No.	Acid Injection Mode	Alternative Stages	Temperature, °C			Acid Volume, L		
			SG Acid	C Acid	G Acid	SG Acid	C Acid	G Acid
1	FF + SG acid	/	75	/	/	31		
2	FF + C acid	/	/	75	/	31		
3	FF + SG acid +C acid (one stage)+ G acid	1	75	63	62	12	18	1
4	FF + SG acid +C acid (two stages)+ G acid	2	85	75	/	6	9	1
			65	63	62	6	9	
5	FF + SG acid +C acid (three stages)+ G acid	3	95	80	/	4	6	1
			70	65	/	4	6	
			65	65	62	4	6	

2.3.3. Experimental Schedule

Based on the confirmed experimental acid-injection rate, time, and reaction temperature, the designed acid-etching fracture scheme is shown in Table 3. Experiments 1 and 2 simulate the effects of the single self-generating acid and cross-linked acid system on the acid-etching behavior. Experiments 3, 4, and 5 simulate the acid-etching behavior of fracturing fluid + self-generating acid + cross-linked acid + gelled acid (closed acidizing) under different alternate stages.

The Yijianfang Formation reservoir depth in the Fuman Oilfield ranges from 6500 m to 8200 m, with the closure pressure ranging from 40 MPa to 80 MPa. Sequential experiments were conducted on the acid-etching fracture followed by laser scanning to analyze the acid-etched fracture morphology. Conductivity tests were performed at intervals of increasing closure pressure by increments of 10 MPa until reaching a maximum pressure level of 80 MPa. The experimental procedure is illustrated in Figure 4.

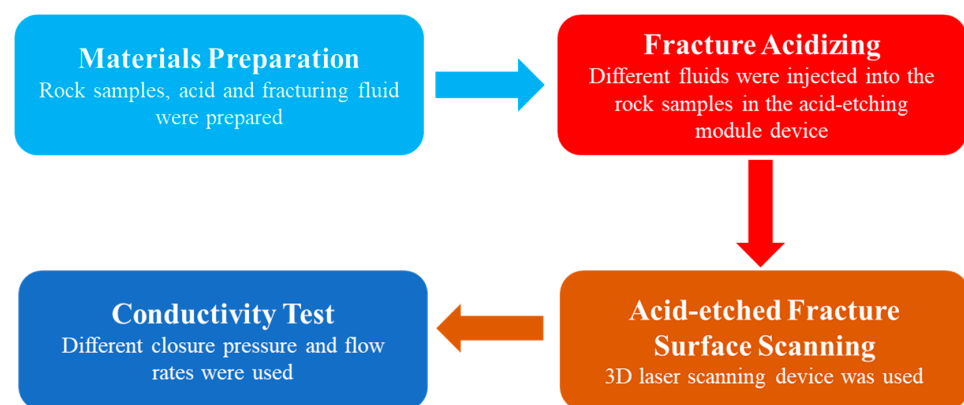


Figure 4. Variation of bottom temperature under different alternate stages.

3. Results and Discussion

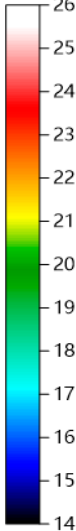
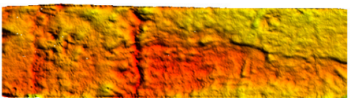
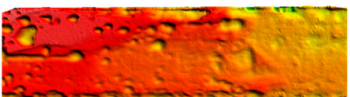
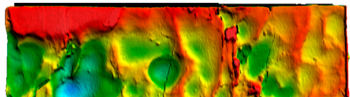
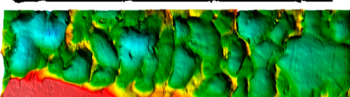
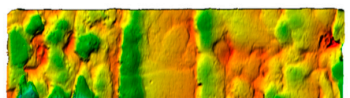
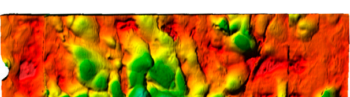
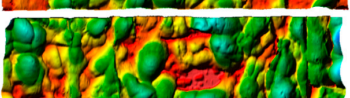
3.1. Characteristics of Acid-Etched Fracture under Different Acid-Injection Modes

Based on the acid-etched fracture morphology and the quantity of rock plate dissolution, we investigated the acid-etched morphology, the distribution of fracture elevation, as well as the features of acid-rock reaction dissolution under conditions involving single acid injection and different alternating injection stages with various acid systems.

3.1.1. Morphological Changes of Hydraulic Fractures before and after Acid Etching

Table 4 shows the morphological changes of rock slabs before and after acid etching under different acid-injection model conditions. It can be observed from Table 4 that prior to acid etching, all rock slabs exhibit a uniformly smooth surface. The presence of bedding and texture variations in the rock samples was attributed to the influence of their respective bedding and joint characteristics.

Table 4. Changes of acid-etching fracture morphology under different acid-injection modes.

Acid-Injection Mode	Before Acid Injection	After Acid Injection	Height Colorimetric Bars
FF + SG acid			<p>Height, mm</p> 
			
FF + C acid			
			
FF + SG acid + C acid (one stage) + G acid			
			
FF + SG acid + C acid (two stages) + G acid			
			
FF + SG acid + C acid (three stages) + G acid			
			

When using the fracturing fluid in conjunction with self-generating acid-injection mode (FF + SG acid), a vertical groove emerged within the central region of the lower rock sample, perpendicular to the direction of acid flow. In the upper rock sample, erosion pits predominantly manifested near the inlet end within the middle section. This indicated that under this injection mode, the rock samples exhibited some degree of non-uniform etching, but the extent of non-uniform etching was relatively minimal. The underlying reason for this alteration was attributed to the limited reactive capacity of the self-generating acid, leading to restricted etching effects on the rock formation [17].

When utilizing the fracturing fluid in conjunction with cross-linked acid-injection mode (FF + C acid), noticeable non-uniform etching was observed on the rock samples. Point-like pits were present near the outlet end of the upper rock surface, while multiple grooves perpendicular to the direction of acid flow were evident on the lower rock surface. Following exposure to cross-linked acid alone, a predominant green coloration was observed on the lower rock plate, whereas the upper rock plate exhibited a predominantly red–green appearance, indicating more severe etching on the lower rock plate. Overall, compared to the injection mode of FF+SG acid, the injection mode of FF+C acid demonstrated a significantly stronger etching capability.

When employing the injection mode of fracturing fluid combined with self-generating acid and cross-linked acid, namely FF + SG acid + C acid (one-three stages) + G acid, the rock face appeared smooth prior to etching. However, after etching, varying degrees of etched grooves emerged on both upper and lower rock plates. In certain regions, natural fractures were formed alongside acid wormholes. As the alternating stage of the injection pattern increased from one to two, distinct fish-scale non-uniform morphology was observed on the rock sample after etching, which may be attributed to the obvious network filling fractured before etching. Furthermore, when the injection stage was increased to three, a more conspicuous fish-scale etching pit was formed.

Comparing the acid-etching morphological characteristics of hydraulic fractures under five different acid-injection processes, it was evident that the acid-etching extent was limited when employing the simple injection mode of fracturing fluid and acid. However, with the alternating injection mode of fracturing fluid and acid, the non-uniform dissolution of rock samples was significantly enhanced. Additionally, features such as dissolution grooves and pits appeared, and the acid fluid obviously communicated potential natural fractures and cavities.

3.1.2. Elevation Frequency Distribution Characteristics of Acid-Etched Rock Slabs

To analyze the impact of different acid-injection processes further quantitatively on acid-etched fracture behavior, the elevation frequency distribution of rock surfaces was selected for the quantitative characterization and analysis of the fracture surfaces before and after acid etching [27]. Elevation frequency distribution refers to the frequency of occurrence of heights at various points on the rock sample surface within a certain range. The histogram and its curve of the elevation frequency distribution visually depict the roughness of the rock sample surface.

Figure 5 illustrates the elevation frequency distribution characteristics after acid etching of rock plates under different acid-injection conditions. The elevation distribution range resulting from the two-stage alternating etching exhibited the widest span, indicating a stronger degree of non-uniform etching. In contrast, the elevation distribution range of the fracturing fluid + single acid-injection mode was narrower, with elevations mostly concentrated in the interval greater than or equal to 20 mm. This suggested that the etching extent of the fracturing fluid + single acid-injection mode was also lower compared to that of the fracturing fluid + multiple acid types alternating injection.

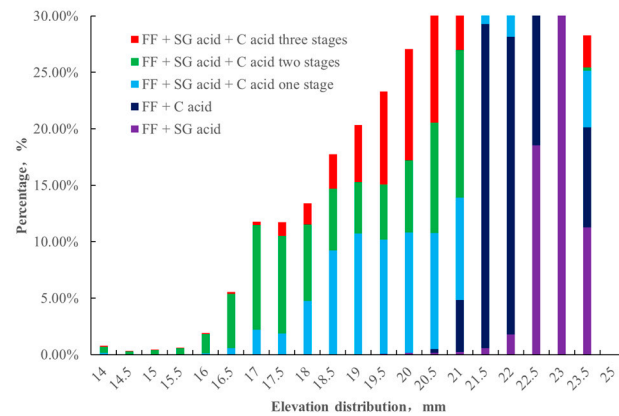


Figure 5. Elevation frequency distribution of acid-etched rock slabs under different acid-injection modes.

Figure 6 presents the cumulative frequency distribution of elevation for acid-etched rock plates under different acid-injection modes. Furthermore, it was observed that the frequency distribution of the rock plates etched with the fracturing fluid + single acid-injection mode was relatively narrow, and the frequency distribution curve exhibited a distinct steep characteristic, indicating a weaker degree of non-uniform etching in the acid-etched morphology. In contrast, the cumulative distribution curves of elevation frequency for acid-etched fracture surfaces formed by the fracturing fluid + different acid-injection modes were relatively flatter, with a broader distribution range. Among them, the elevation distribution curve formed by the two-stage alternating injection mode was the widest and flattest, indicating a stronger degree of non-uniform etching, consistent with the results in Table 4.

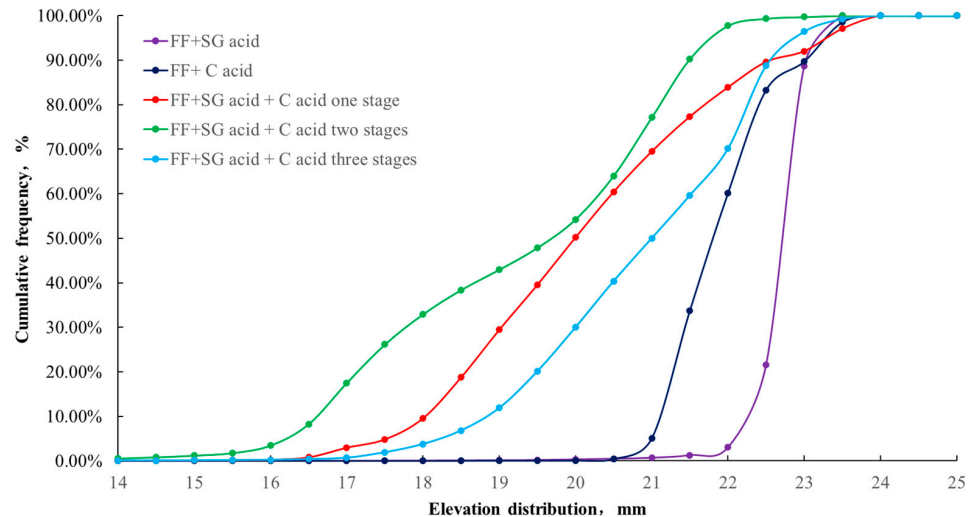


Figure 6. Cumulative frequency distribution of acid-etched slab elevation under different acid-injection modes.

3.1.3. Acid-Rock Reaction Characteristics

The overall acid dissolution quantity of the rock plates reflected the degree of acid-rock reaction during each set of acid-etching experiments. A higher dissolution quantity indicated a greater amount of rock consumed in the acid-etching process, which suggested a more intense acid-rock reaction. Figure 7 displays the variation in acid-dissolution quantity of rock plates under different acid-injection conditions. It is evident that the rock plates under two-stage alternating injection mode resulted in larger quantities of dissolved rock, indicating more intense and non-uniform etching. This non-uniform etching enhanced the roughness of the acid-etched fracture surface, thereby augmenting the area for the

acid-rock reaction and consequently resulting in an escalation of corrosion. This substantial level of acid-induced corrosion and the extent of non-uniform etching were mutually reinforcing. This finding is consistent with the numerical characterization of acid etching and the elevation frequency distribution features in Table 4 and Figures 5 and 6.

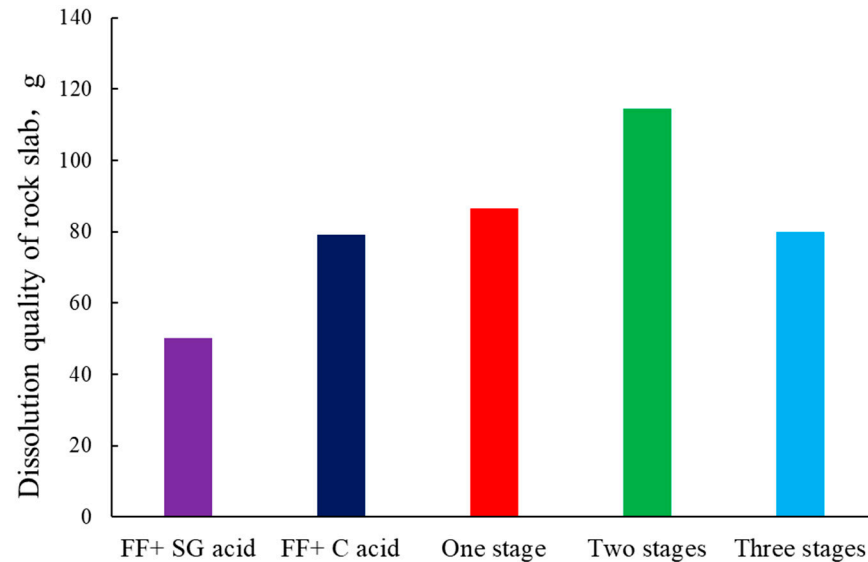


Figure 7. Amount of dissolution of slabs with different acid-injection modes.

3.2. Variation Characteristics of Fracture Conductivity under Different Acid-Injection Modes

In order to reveal the variation of the acid-etched fracture conductivity, the retention rate of conductivity at a certain closure stress is defined as the percentage of the conductivity in the initial conductivity by Equation (2) [17]:

$$R = \frac{(Kw)_i}{(Kw)_o} \times 100\% \quad (2)$$

where R is the conductivity retention rate, %; $(Kw)_i$ is the conductivity under closure stress i , D·cm; and $(Kw)_o$ is the initial conductivity, D·cm.

Figures 8 and 9 illustrate the variations in acid-etched fracture conductivity and conductivity retention rate under different acid systems and alternating injection modes.

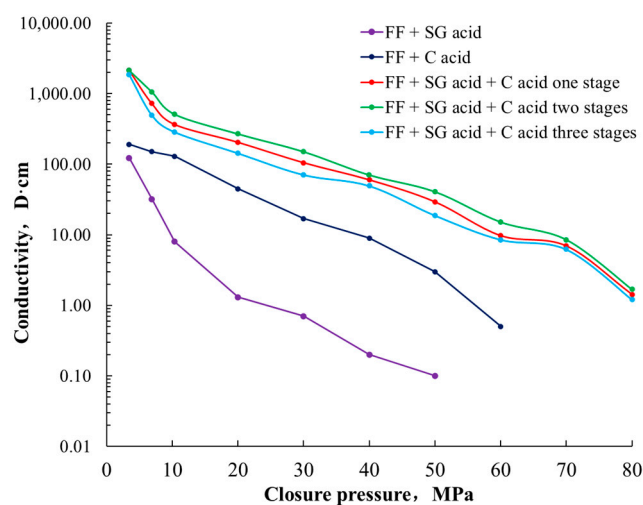


Figure 8. Conductivity under different acid-injection modes.

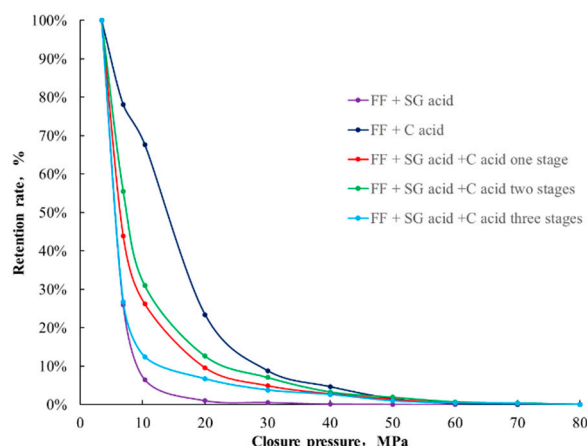


Figure 9. Comparison of changing rates of conductivity under different acid-injection modes.

Based on Figures 8 and 9, it is evident that significant differences exist in the conductivity and conductivity retention of acid-etched fractures under varying acid-injection conditions. In terms of conductivity, when the closure pressure was less than or equal to 60 MPa, the overall trend indicated that the conductivity under the alternating acid-injection mode was greater than that under the fracturing fluid + single acid-injection mode. Moreover, consistently displaying superior values, the two-stage alternating injection mode demonstrated optimal conductivity levels. When the closure pressure exceeded 60 MPa, the effectiveness of the fracturing fluid + single acid-injection mode in maintaining conductivity diminished significantly. Therefore, considering the conductivity factor, it was not advisable to employ the fracturing fluid + single acid-injection mode as pre-acid fracturing for deep carbonate reservoirs in the Fuman Oilfield.

Regarding conductivity retention, when the closure pressure was greater than 10 MPa, the acid-etched fracture conductivity was less than 50% of its initial value. This suggested that under the influence of normal closure pressure conditions, the acid-etched fracture gradually came into contact and consolidation, resulting in compression and reduction of the fracture flow channel. When the closure pressure exceeded 20 MPa, there was no significant change in conductivity retention rate. Overall, the mode of fracturing fluid + cross-linked acid exhibited a higher retention rate of conductivity, indicating a stronger ability of the acid-etched fracture to resist deformation under normal closure pressure. However, on the other hand, as indicated by Figure 8, when the closure pressure exceeds 60 MPa, the conductivity formed by the fracturing fluid + single acid-injection mode has essentially been lost. The reasons for the loss of conductivity under high closure stress are as follows: first, complete contact between the rock faces leaves no seepage space available; another contributing factor may be the significant deterioration in mechanical strength of rock samples during the acidizing process [28,29], leading to detachment and migration of mineral particles that gradually accumulate at fracture outlets, thereby impeding accurate measurement of conductivity. This phenomenon also occurs in real-life mining scenarios [30]. The comprehensive consideration of conductivity suggested that the two-stage alternating injection mode of fracturing fluid + acid was recommended for acid fracturing in deep carbonate reservoirs in the Fuman Oilfield.

4. Field Application

The 305H well is an appraisal well located in the Fuman Oilfield, with the target interval for stimulation being 7763.00–8410.00 m. During drilling, the well encountered a fracture-cavity body boundary directly (Figure 10). The spatial relationship between the wellbore and reservoir body is as follows: vertically, the initiation point of the fractures is 108 m away from the core of the cavity in the upward fracture height direction, 180 m away from the boundary of the cavity, and 10 m away from the boundary in the downward fracture height direction (Figure 10a). Horizontally, the cavity body extends in a northeast

direction, similar to the direction of fracture propagation. Along the direction of fracture propagation, the initiation point is 134–202 m away from the cavity boundary and 104 m away from the core of the cavity (Figure 10b).

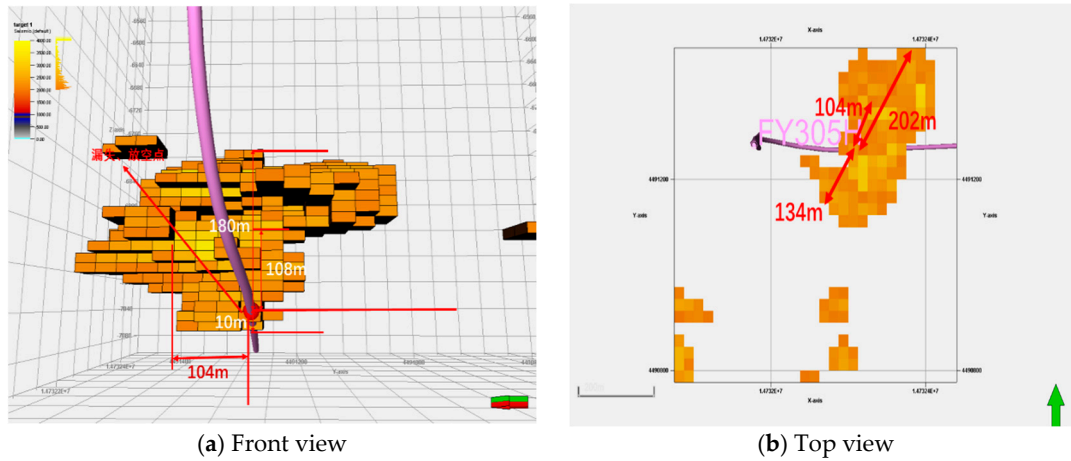


Figure 10. The relationship between fracture-cavity and wellbore position in 305H well.

To ensure effective communication with the cavity body by employing acid fracture, there is a significant demand for the upper fracture height, which should be greater than 108 m, and the fracture length should be greater than 104 m. Figure 11 illustrates the variation in fracture geometry parameters calculated using fracturing simulation software 1.0 under different injection rates and injection volumes. To guarantee effective communication with the cavity body, it was recommended to use an injection displacement of $\geq 6.0 \text{ m}^3/\text{min}$ and an injection volume of 1200–1400 m^3 .

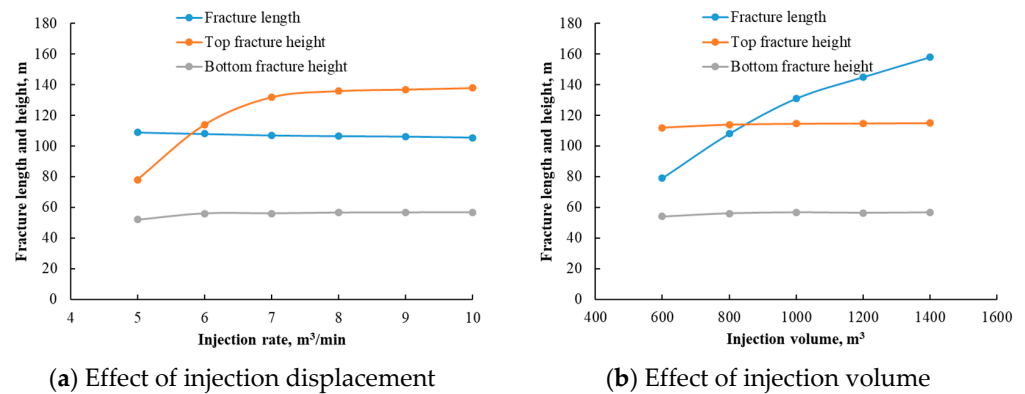


Figure 11. Influence of different injection parameters on geometric size of acid-fractured fracture.

Based on the experimental results of acid-etched fracture conductivity, the recommended acid fracturing injection mode was the two-stage alternating injection of FF + SG acid + C acid, followed by gelled acid for closed acidizing. According to the designed total injection volume of 1200–1400 m^3 , the individual fluid volumes were as follows: fracturing fluid 390 m^3 , gelled acid 200 m^3 , self-generating acid 380 m^3 , cross-linked acid 400 m^3 , and displacement fluid 80 m^3 .

The well successfully underwent a two-stage alternating acid-fracturing treatment in accordance with the design parameters (Figure 12). The shutdown tubing pressure curve depicted in Figure 12 appears to be nearly linear, which is a typical response of an acid-fracture communication pressure response for a large fracture cavity [31]. This indicates that the design objective for acid fracturing has been successfully achieved.

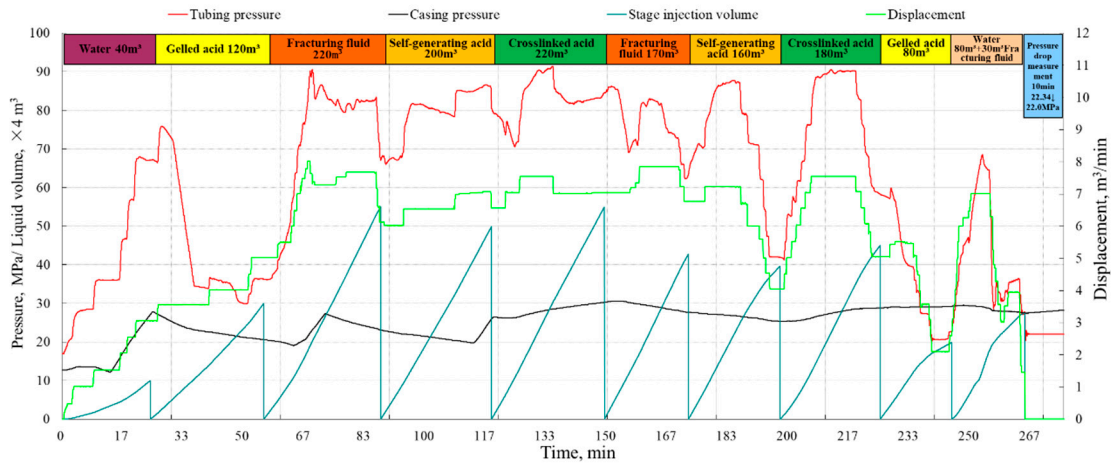


Figure 12. Construction curve of acid fracturing in FY305H well.

Following the acid-fracturing treatment, the daily oil production has reached 240 m³/d, while the daily gas production stands at 85,686 m³/d, resulting in an equivalent oil production rate of 265.6 t/d. This signifies a remarkable increase in production by 20.4% compared to neighboring wells employing three-stage alternating acid fracturing under similar conditions listed in Table 5. Furthermore, it is worth noting that the acid-injection process has been streamlined.

Table 5. Comparison of acid-injection parameters and production from test well and adjacent well.

Well	Fracturing Fluid m ³	Cross-Linked Acid m ³	Self-Generating Acid m ³	Gelled Acid m ³	Acid-Injection Mode	Equivalent Oil Production Rate t/d
305H	390	400	380	200	two stages	265.6
701	760	410	300	50	three stages	220.6

5. Proposal for Future Improvements

Although this paper conducted experimental research on the conductivity of different acid-injection modes, there are still several future research suggestions:

- (1) The enhancement of rock pore and natural fracture permeability through acid solution should be prioritized, along with its subsequent impact on conductivity. The acid fluid infiltrates the rock pores and the natural fractures on the fracture wall during acid fracturing, lead to pore enlargement in the reservoir and increased width of natural fractures through acid dissolution. As a result, permeability is enhanced.
- (2) The influence of rough hydraulic morphology and changes in rock mechanical strength on conductivity should be further emphasized, and a corresponding model for predicting conductivity should be established. This is also crucial for the design of acid pressure schemes and evaluating their effectiveness.

6. Conclusions

- (1) The non-uniform etching degree of the hydraulic fractures is less pronounced in the fracturing fluid + single acid-injection mode compared to that under the fracturing fluid + multiple types of acid alternating injection mode. Furthermore, an increasing trend in the non-uniform etching degree is observed with an increase in injection stages. However, the two-stage alternating injection mode exhibits a higher degree of non-uniform etching.
- (2) Conductivity generated under the fracturing fluid + multiple types of acid alternating injection mode is superior to that produced under the fracturing fluid + single acid-injection mode.

- (3) From the perspective of conductivity, it is recommended to adopt the fracturing fluid + different types of acid alternating injection mode based on the closure pressure characteristics of the Fuman Oilfield. Field application results indicate significantly improved production enhancement and stimulation effects using this acid-injection mode.

Author Contributions: Writing—draft and investigation—experimental, J.L. (Jiangyu Liu); Investigation—discussion, D.R.; Conceptualization—S.F. and J.L. (Ju Liu); Investigation—field application and discussion, S.Q. and X.Q.; Reviewing and Conceptualization, B.G. All authors have read and agreed to the published version of the manuscript.

Funding: This research received no external funding.

Data Availability Statement: Data sharing is provided as required.

Conflicts of Interest: Authors Jiangyu Liu, Dengfeng Ren, Shaobo Feng, Ju Liu, Shiyong Qin and Xin Qiao were employed by the company PetroChina. The remaining author declares that the research was conducted in the absence of any commercial or financial relationships that could be construed as a potential conflict of interest.

References

- He, D.F.; Jia, C.Z.; Zhao, W.Z.; Xu, F.Y.; Luo, X.R.; Liu, W.H.; Tang, Y.; Gao, S.L.; Zheng, X.J.; Li, D.; et al. Research progress and key issues of ultra-deep oil and gas exploration in China. *Pet. Explor. Dev.* **2023**, *50*, 1162–1172. [[CrossRef](#)]
- Lei, Q.; Xu, Y.; Yang, Z.W.; Cai, B.; Wang, X.; Zhou, L.; Liu, H.F.; Xu, M.J.; Wang, L.W.; Li, S. Progress and development directions of stimulation techniques for ultra-deep oil and gas reservoirs. *Pet. Explor. Dev.* **2021**, *48*, 193–201. [[CrossRef](#)]
- Aljawad, M.S.; Aljulaih, H.; Mahmoud, M.; Desouky, M. Integration of field, laboratory, and modeling aspects of acid fracturing: A comprehensive review. *J. Pet. Sci. Eng.* **2019**, *181*, 106158. [[CrossRef](#)]
- Deng, J.; Mou, J.; Hill, A.D.; Zhu, D. A new correlation of acid-fracture conductivity subject to closure stress. *SPE Prod. Oper.* **2012**, *27*, 158–169. [[CrossRef](#)]
- Zhang, L.; Zhou, F.; Mou, J.; Xu, G.; Zhang, S.; Li, Z. A new method to improve long-term fracture conductivity in acid fracturing under high closure stress. *J. Pet. Sci. Eng.* **2018**, *171*, 760–770. [[CrossRef](#)]
- Bale, A.; Smith, M.B.; Klein, H.H. Stimulation of carbonates combining acid fracturing with proppant (CAPF): A Revolutionary Approach for Enhancement of Sustained Fracture Conductivity and Effective Fracture Half-length. In Proceedings of the SPE Annual Technical Conference and Exhibition, Florence, Italy, 20–22 September 2010.
- Desouky, M.; Samarkin, Y.; Aljawad, M.S.; Amao, A.; AlTammar, M.J.; Alruwaili, K.M. Diammonium Phosphate Treatment for Sustained Hydraulic/Acid Fracture Conductivity in Chalk and Limestone Formations. *SPE J.* **2024**, 1–13. [[CrossRef](#)]
- Desouky, M.; Aljawad, M.S.; Abduljamiu, A.; Solling, T.; Abdulaheem, A.; AlTammar, M.J.; Alruwaili, K.M. Enhancing Fracture Conductivity in Soft Chalk Formations with Diammonium Phosphate Treatment: A Study at High Temperature, Pressure, and Stresses. *SPE J.* **2023**, *28*, 3280–3290. [[CrossRef](#)]
- Coulter, A.W.; Crowe, C.W.; Barrett, N.D.; Miller, B.D. Alternate stages of pad fluid and acid provide improved leakoff control for fracture acidizing. In Proceedings of the Society of Petroleum Engineers (SPE), New Orleans, LA, USA, 3 October 1976.
- Li, X.; Chen, Y.; Yang, Z.; Chen, F. Large-scale visual experiment and numerical simulation of acid fingering during carbonate acid fracturing. In Proceedings of the SPE Asia Pacific Oil and Gas Conference and Exhibition, Jakarta, Indonesia, 17–19 October 2017.
- Li, X.; He, Y.; Yang, Z.; Zhu, J.; Li, F.; Song, R. Fully coupled model for calculating the effective acid penetration distance during acid fracturing. *J. Nat. Gas Sci. Eng.* **2020**, *77*, 103267. [[CrossRef](#)]
- Jiao, F.Z. Practice and knowledge of volumetric development of deep fractured-vuggy carbonate reservoirs in Tarim Basin, NW China. *Pet. Explor. Dev.* **2019**, *46*, 576–582. [[CrossRef](#)]
- Petruz Munguia, J.M.; Gonzalez Valtierra, B.E.; Trujillo Hernandez, J.; Santos, S.; Campos Monroy, K. Acid-fracturing techniques as a good alternative to help improve field development assets. In Proceedings of the Abu Dhabi International Petroleum Exhibition and Conference, Abu Dhabi, United Arab Emirates, 11–14 November 2019.
- Sarma, D.K.; Pal, T.; Kumar, D.; Lahiri, G.; Manchalwar, V.V. Application of Closed Fracture Acidizing for Stimulation of Tight Carbonate Reservoir in Mumbai Offshore. In Proceedings of the SPE Oil and Gas India Conference and Exhibition, Mumbai, India, 4–6 April 2017.
- Mou, J.Y.; Zhang, S.C. Modeling acid leakoff during multistage alternate injection of pad and acid in acid fracturing. *J. Nat. Gas. Sci. Eng.* **2015**, *26*, 1161–1173. [[CrossRef](#)]
- Zhang, K.; Chen, M.; Zhou, C.; Dai, Y.; Liu, F.; Li, J. Study of alternating acid fracturing treatment in carbonate formation based on true tri-axial experiment. *J. Pet. Sci. Eng.* **2020**, *192*, 107268. [[CrossRef](#)]
- Gou, B.; Guan, C.C.; Li, X.; Ren, J.C.; Zeng, J.; Wu, L.; Guo, J.C. Acid-etching fracture morphology and conductivity for alternate stages of self-generating acid and gelled acid during acid-fracturing. *J. Pet. Sci. Eng.* **2021**, *200*, 108358. [[CrossRef](#)]
- Zhang, Q.; Liu, P.; Xiong, Y.; Du, J. Self-Generated Organic Acid System for Acid Fracturing in an Ultrahigh-Temperature Carbonate Reservoir. *ACS Omega* **2023**, *8*, 12019–12027. [[CrossRef](#)]

19. Lungwitz, B.; Fredd, C.; Brady, M.; Miller, M.; Ali, S.; Hughes, K. Diversion and cleanup studies of viscoelastic surfactant-based self-diverting acid. *SPE Prod. Oper.* **2007**, *22*, 121–127. [[CrossRef](#)]
20. Navarrete, R.C.; Holms, B.A.; McConnell, S.B.; Linton, D.E. Laboratory, theoretical, and field studies of emulsified acid treatments in high-temperature carbonate formations. *SPE Prod. Facil.* **2000**, *15*, 96–106. [[CrossRef](#)]
21. Tariq, Z.; Hassan, A.; Al-Abdrabalnabi, R.; Aljawad, M.S.; Mahmoud, M. Comparative study of fracture conductivity in various carbonate rocks treated with GLDA chelating agent and HCl acid. *Energy Fuels* **2021**, *35*, 19641–19654. [[CrossRef](#)]
22. Sui, Y.; Cao, G.; Guo, T.; Li, Z.; Bai, Y.; Li, D.; Zhang, Z. Development of gelled acid system in high-temperature carbonate reservoirs. *J. Pet. Sci. Eng.* **2022**, *216*, 110836. [[CrossRef](#)]
23. Ren, Y.; Wang, D.; Feng, P.; Chen, J.; Shao, S.; Zhang, W.; Cui, B. An Integrated Experimental Method to Study Multistage Alternating Injection Acid Fracturing in Limestone Formation. In Proceedings of the SPE Middle East Oil and Gas Show and Conference, Manama, Bahrain, 9–21 February 2023.
24. Zhu, D.; Wang, Y.; Cui, M.; Zhou, F.; Wang, Y.; Liang, C.; Yao, F. Acid system and stimulation efficiency of multistage acid fracturing in porous carbonate reservoirs. *Processes* **2022**, *10*, 1883. [[CrossRef](#)]
25. Wang, Q. Origin of gas condensate reservoir in Fuman Oilfield, Tarim Basin, NW China. *Pet. Explor. Dev.* **2023**, *50*, 1128–1139. [[CrossRef](#)]
26. Guo, J.C.; Liu, Z.; Gou, B.; Zeng, M.Y. Study of wellbore heat transfer considering fluid rheological effects in deep well acidizing. *J. Pet. Sci. Eng.* **2020**, *191*, 107171. [[CrossRef](#)]
27. Gou, B.; Li, X.; Ma, H.Y.; Zhou, C.L. Effects of Morphology of Hydraulic Fractures on Acid Etching Behaviors and Fluid Diversion Capacity. *J. Southwest Pet. Univ.* **2019**, *41*, 80–90.
28. Jin, S.; Wang, X.; Wang, Z.; Mo, S.; Zhang, F.; Tang, J.; Xiong, H. Evaluation approach of rock brittleness index for fracturing acidizing based on energy evolution theory and damage constitutive relation. *Lithosphere* **2021**, *2021*, 2864940. [[CrossRef](#)]
29. Chen, W.; Yang, J.; Li, L.; Wang, H.; Huang, L.; Jia, Y.; Hu, Q.; Jiang, X.; Tang, J. Investigation of Mechanical Properties Evolution and Crack Initiation Mechanisms of Deep Carbonate Rocks Affected by Acid Erosion. *Sustainability* **2023**, *15*, 11807. [[CrossRef](#)]
30. Grifka, J.; Nehler, M.; Licha, T.; Heinze, T. Fines migration poses challenge for reservoir-wide chemical stimulation of geothermal carbonate reservoirs. *Renew. Energy* **2023**, *219*, 119435. [[CrossRef](#)]
31. Chen, Z.; Zhang, S. Evaluation of geological effects of acid-fracturing in deep carbonate reservoirs: Taking the fractured-vuggy carbonate reservoirs in Tahe oilfield as an example. *Oil Gas Geol.* **2004**, *25*, 686–691.

Disclaimer/Publisher's Note: The statements, opinions and data contained in all publications are solely those of the individual author(s) and contributor(s) and not of MDPI and/or the editor(s). MDPI and/or the editor(s) disclaim responsibility for any injury to people or property resulting from any ideas, methods, instructions or products referred to in the content.